

## CANCELING STRONG NARROWBAND MAIN-BEAM INTERFERENCE

A. A. (Louis) Beex  
DSPRL – ECE 0111  
Virginia Tech  
Blacksburg, VA 24061-0111, USA

& James R. Zeidler  
Communications & Information Systems, 28505  
SPAWAR Systems Center  
San Diego, CA 92152, USA

### Abstract

In a generalized sidelobe canceler using normalized least mean square adaptation, interference coming in on sidelobes can be mitigated when using a small adaptation stepsize. In that case, any interference arriving from the main beam look direction will be viewed as a desirable signal, and therefore passed on. Previous studies have identified narrowband interference scenarios where interference mitigation is enhanced by non-Wiener effects in normalized least mean square adaptive filtering using existing filter structures. In this paper we seek to further extend narrowband interference mitigation by expanding the adaptive filtering structures to better utilize the information responsible for non-Wiener effects. While in the generalized sidelobe canceler adaptation takes place in the spatial domain of auxiliary beams, here we seek to incorporate the temporal dimension as well. The latter will be applied to the auxiliary beams and the main beam, or to the error signal of the generalized sidelobe canceler. The performance of the space-time adaptive processor operating on the temporal signals from the main beam and auxiliary beams simultaneously turns out to be comparable to that of a temporal smoothing stage operating on the generalized sidelobe canceler error.

### KEY WORDS

Narrowband Interference Mitigation, Non-Wiener Effects, Dynamic Weight Behavior, NLMS, Multi-Stage Adaptive Filter, Space-Time Adaptive Processing.

### 1. Introduction

One of the problems encountered in communicating wideband signals is the existence of narrowband interference. For many wideband signals of interest the narrowband interference is stronger than the signal itself. When the signal of interest (SOI) arrives from a given direction, the look direction, interference from other directions can be effectively reduced using the generalized sidelobe canceler (GSC). As the signal of interest is relatively weak, it is conceivable that the main beam signal consists of a wideband signal of interest contaminated by strong narrowband interference [1], for example as the result of a satellite transponder operating in nonlinear mode [2].

In the GSC a main beam antenna pattern is chosen so that the signal of interest, from the direction of interest, is separated from the signals impinging from other directions. In particular, the auxiliary beams have a null in the direction of the signal of interest. We implement the GSC as an adaptive filter, and concentrate on using the normalized least mean square (NLMS) algorithm for adaptation. The latter facilitates the adaptive combining of the auxiliary beam signals in such a way that signals not arriving from the look direction can be reduced or even canceled. As in most adaptive filtering scenarios, the performance and realm of applicability of the GSC approaches that of the associated Wiener filter.

Signal distortion or cancellation in adaptive array processing is usually the result of leakage of the signal [3, 4] into the auxiliary beams. If the main beam interferer leaks into the auxiliary beams, that leakage can be used to cancel the main beam interference. The latter leads to signal distortion, because the signal of interest and the main beam interferer are both coming from the same direction and the adaptive filter will primarily aim at canceling the strong interferer. A potential solution to the signal distortion problem is to use *postbeamformer interference cancellation* (PIC) [4], which amounts to creating an essentially signal-free reference (or auxiliary beam) by looking in the interferer direction with a separate beamformer. This is not physically possible in our case because the desired signal and main beam interferer are coming from the same source direction. Presumably our SOI is inherently contaminated and there is no leakage problem, so that the main beam interferer is not present in any of the auxiliary beams.

When narrowband signals and NLMS are involved, the realm of applicability of the adaptive GSC is extended as a result of non-Wiener effects. The latter may be characterized by improved performance relative to the corresponding Wiener filter scenario and by dynamic weight behavior [5]. The latter effects occur in the classically used GSC setting under a change in adaptation step size, from classically small to approaching even the maximal step size of one. The explanation for the resulting non-Wiener performance leads to a further expansion of the realm of applicability, this time by generalizing the structure of the adaptive filter itself in order to more fully utilize the information that can lead to non-Wiener effects.

In Section 2 the fundamental GSC setup is reviewed in the context of the problem of interest. In Section 3 we show the enlargement of the realm of applicability when using NLMS adaptation, and review the operation expected under Wiener filter operation. The latter leads us to propose, in Section 4, a stage of temporal smoothing in addition to the spatial processing notions of main and auxiliary beams of the GSC. In Section 5 spatial and temporal processing of the main and auxiliary beam signals is combined in a single stage of adaptation, and its performance compared to that of two-stage GSC error smoothing approach in the scenario with narrowband interference on a wideband signal of interest that is the subject of this investigation.

## 2. GSC Setup

The signal  $y_n$  impinging on a three-element linear sensor array, consists of a wideband signal of interest  $q_n$ , which is a QPSK signal with power one impinging from broadside, a sinusoidal interferer with fractional frequency 0.03 impinging from a  $30^\circ$  angle with respect to broadside, an order one autoregressive interferer  $a_n$  impinging from broadside, and white Gaussian sensor noise.

$$y_n = q_n + s_n + a_n + v_n \quad (1)$$

The AR(1) interferer is narrowband (NB), characterized by its pole, as given here.

$$\begin{aligned} a_n &= p_a a_{n-1} + e_n \\ p_a &= 0.999 \exp(2\pi j 0.035) \end{aligned} \quad (2)$$

The signal-to-interference-ratio, SIR, is set to  $-25$  dB for the sinusoidal interferer as well as for the AR(1) interferer, while the signal-to-noise-ratio, SNR, is set to 20 dB ( $\frac{\sigma_q^2}{\sigma_s^2}$ ,  $\frac{\sigma_q^2}{\sigma_a^2}$ , and  $\frac{\sigma_q^2}{\sigma_v^2}$  respectively). The generalized sidelobe canceler scenario of interest is shown in Fig. 1.

The desired signal for NLMS adaptation,  $d_n$ , is derived from the quiescent weight vector  $\mathbf{w}_q$  operating on  $\mathbf{y}_n$ , the vector of sensor signals. The reference input vector for NLMS adaptation,  $\mathbf{x}_n$ , comes from the operation of the signal blocking matrix  $\mathbf{C}_a$  on  $\mathbf{y}_n$ . The overall GSC weight vector  $\mathbf{w}_n$  can be expressed as follows.

$$\mathbf{w}_n = \mathbf{w}_q - \mathbf{C}_a \mathbf{w}_{a,n} \quad (3)$$

The blocking matrix satisfies  $\mathbf{C}^H \mathbf{C}_a = \mathbf{0}$ , where the constraint matrix  $\mathbf{C}$  is determined by any linear constraints imposed on the GSC as follows.

$$\mathbf{C}^H \mathbf{w}_n = \mathbf{g} \quad (4)$$

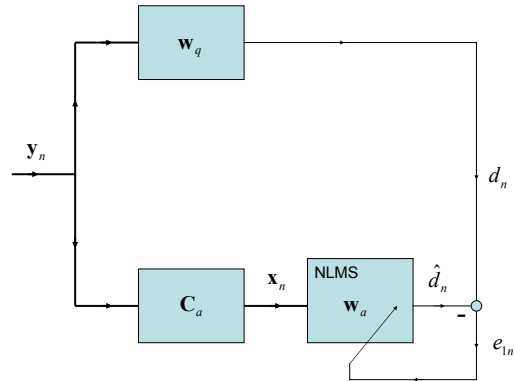


Fig. 1: GSC Setup.

In our example, there is a single linear constraint, which ensures that the array gain in the look direction, broadside, equals one, while allowing the adaptation to proceed in an unconstrained manner. As we have three array elements, there will thus be two auxiliary beams.

The adaptation of interest is the normalized least mean square algorithm, which for the GSC setup above is implemented as follows.

$$\begin{aligned} \mathbf{w}_{a,n+1} &= \mathbf{w}_{a,n} + \mu \frac{e_{1n}^*}{\mathbf{x}_n^H \mathbf{x}_n} \mathbf{x}_n \\ e_{1n} &= d_n - \hat{d}_n \\ d_n &= \mathbf{w}_q^H \mathbf{y}_n \\ \hat{d}_n &= \mathbf{w}_{a,n}^H \mathbf{x}_n \\ \mathbf{x}_n &= \mathbf{C}_a^H \mathbf{y}_n \end{aligned} \quad (5)$$

The orthogonal nature of the main beam with respect to the auxiliary beams, implies that the sinusoidal interferer must be present in one or more of the auxiliary beams. Consequently, the adaptive filter can successfully cancel the sinusoidal component from the desired signal, as provided by the main beam. Note however, that in our scenario, in addition to the QPSK signal-of-interest (SOI), there is also a strong narrowband component impinging from the look direction. Due to the orthogonal nature of the auxiliary beams with respect to the main beam, there is no information in the auxiliary beams related to the signals impinging on the array from the look direction. The Wiener filter solution to the problem at hand is therefore that minimization of the GSC error  $e_{1n}$  occurs when the GSC error approaches SOI+AR(1)+residual noise. For the present scenario, where SIR= $-25$  dB, this means that a simple (minimum distance to an original symbol) detector can not recover the SOI from its best estimate,  $e_{1n}$ . In theory then, we expect a symbol-error-rate (SER) of 0.75 with QPSK as the SOI, as when guessing one of its four possible symbols.

Using an NLMS step size  $\mu = 0.005$  the adaptive GSC performance is expected to approach that of the Wiener GSC. Running the corresponding simulation experiment for 100 realizations, in each of which SER is evaluated over 1000 symbols during steady state operation, produced SER=0.7227. This establishes the Wiener GSC performance benchmark.

When SIR is such that the narrowband interference dominates the SOI, the minimum distance detector can not be successful. As SIR increases, there will be a threshold beyond which SER comes down markedly. The latter loosely defines the realm of Wiener performance, in the context of the present problem.

### 3. NLMS non-Wiener Effect

We have recently shown that in the above scenario a non-Wiener effect may occur, as a result of operating the adaptive filter at a larger step-size than commonly used [5]. Such non-Wiener effects are characterized by performance improvement over that of the corresponding fixed Wiener filter structure and by dynamic rather than (noisily) static weight behavior [6, 7].

In the above scenario, let's change SIR to  $-10$  dB in order to illustrate the non-Wiener effect. Figure 2 shows SER for 100 independent realizations, where SER is estimated from 1000 consecutive symbols during steady-state NLMS operation, for step-sizes of 0.005 and 0.5.

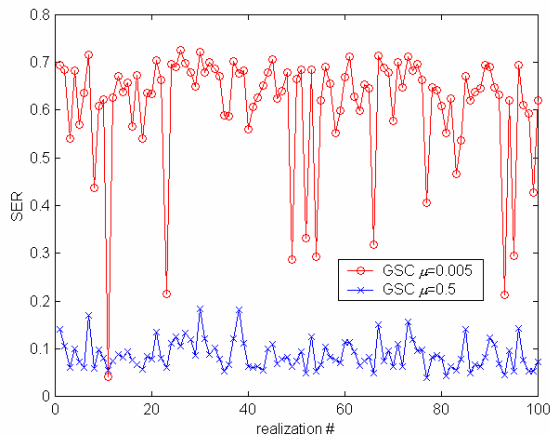


Fig. 2: NLMS GSC SER at SIR=-10 dB.

While we have seen earlier that the non-Wiener effect produced smaller estimation errors, we see here that this can translate into significant SER improvement. The difference in SER for this case is the difference between random guessing, for the small step-size, and a useful digital communication channel, for the large step-size. While an SER around 10% is not small, when it is combined with coding, the non-Wiener effect in the NLMS GSC extends the region where communication is

feasible. We further note that this performance reversal has taken place as the result of a change in parameter only; the hardware and software setup have remained exactly the same.

In addition to performance improvement, the non-Wiener effect is characterized by dynamic weight behavior, as shown in Fig. 3.

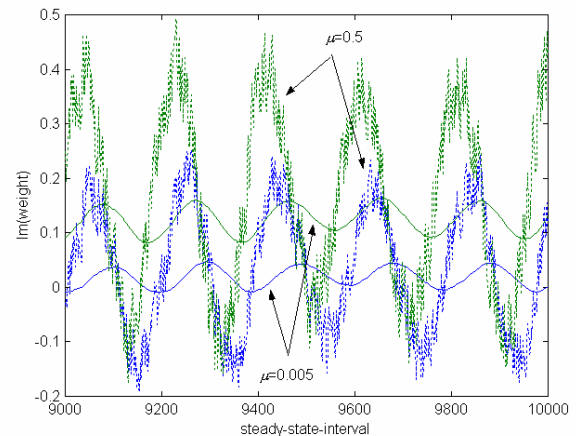


Fig. 3: NLMS GSC dynamic weight behavior.

While there is no statistical information about the AR(1) interference in the main beam present in the auxiliary beams, the adaptive filter weights can serve to modulate the sinusoidal interference in the auxiliary beams and thereby partially cancel that narrowband interference. At large step-size, the NLMS adaptive filter uses the information in the desired signal to find adaptive weights that track the desired signal. As this tracking takes place a posteriori, there is a lag error. As a result, the more narrowband the processes involved, and the closer in temporal frequency, the better the cancellation [7]. We observe in Fig. 3 that while there is dynamic weight behavior at both step-sizes, it is much more pronounced at the larger step-size. In fact, as step-size vanishes, the dynamic weight behavior and the deviations from Wiener performance vanish concurrently.

### 4. GSC Error Smoothing

While the non-Wiener effect in NLMS has afforded us some expansion of the realm of performance for our problem of interest, as the level of the interference increases the level of the lag error also increases. As the QPSK signal power has remained the same, the signal to noise ratio at the input of the detector has decreased, and so does the SER. This deterioration is illustrated in Fig. 4 for SIR=-25 dB. This example shows that, while there is still some increased performance due to a non-Wiener effect, the performance advantage is disappearing. Consequently, another way to increase performance is highly desirable.

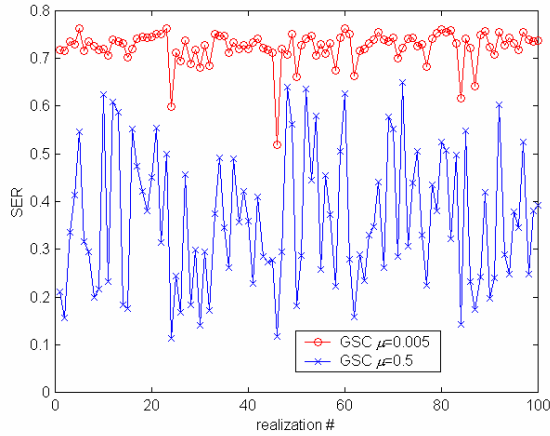


Fig. 4: NLMS GSC SER at SIR=-25 dB.

First, recall that the GSC setup entails orthogonalizing in the spatial domain followed by adaptive filtering in the temporal domain. Second, the spatial filtering itself is very effective. Under the best of circumstances, the Wiener filter perfectly removes the sinusoidal interference from the desired signal, incurring no lag error, and regardless of frequency difference with the narrowband interference. This implies that the GSC error signal itself consists of SOI + NB AR(1) + AWGN, and that this GSC error signal is dominated by the NB AR(1) interference in our scenario. The latter suggests building an estimator for the NB AR(1) interference at some lag, based on GSC errors before and after the lag index. The resulting GSC error smoothing approach is shown in Fig. 5.

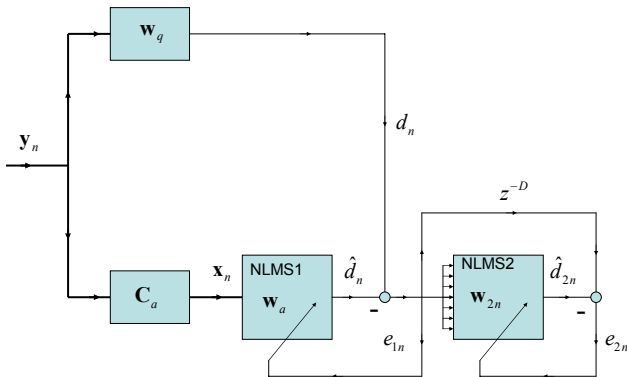


Fig. 5: GSC error smoothing approach.

We use twelve samples before and twelve samples after to produce an estimate of the AR(1) interference at the delay (lag)  $D$  of thirteen. In terms of adaptive filtering, the GSC error signal enters a tapped delay line (TDL) with twenty-five taps and all but the center tap are used to estimate the value at the center tap. Note that the QPSK SOI as well as the AWGN are white, so that these components turn the GSC error process into an ARMA(1,1) (autoregressive-moving average) process. The estimation (smoothing)

process for the latter benefits from using a TDL longer than either of its orders.

The second stage of the multi-stage GSC error smoothing approach produces an error,  $e_{2n}$ , which is an approximation to SOI+AWGN, as long as the original GSC stage approaches Wiener filter behavior. Towards the latter goal, both adaptive filter stages are operated at small step-sizes; in the subsequent example  $\mu = 0.005$ . The SER result is reflected in Fig. 6.

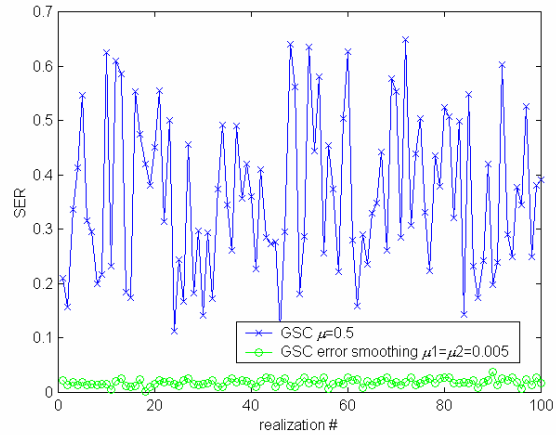


Fig. 6: GSC error smoothing SER.

This simulation experiment used the same data as in the last experiment at SIR=-25 dB, and contrasts the previous SER result with that obtained from the two-stage GSC error smoothing approach. The max SER over all 100 realizations is now 0.0370, while the average SER is 0.0183. We observe that the two-stage GSC error smoothing approach represents a further expansion of the realm for successful detection performance.

## 5. Main-Aux STAP Approach

The multi-stage GSC error smoothing approach uses spatial filtering followed by temporal filtering. Its success is highly suggestive of a single-stage simultaneous space-time adaptive process (STAP). To this end we will use tapped delay lines on the main beam and the auxiliary beams. We again use gapped tapped delay lines, i.e. adaptation does not use the SOI sample value at the delay (lag) time in its input. The main-aux STAP approach is indicated in Fig. 7.

The gapped tapped delay line inputs are concatenated into a single input vector, which is then used in the usual NLMS algorithm. An advantage of this approach is that the information bearing signals, i.e. the main and auxiliary beam signals, are used directly in producing an estimate of SOI+AWGN. The adaptation error signal,  $e_{3n}$ , is again used as the input to the minimum symbol distance detector. A potential disadvantage is that the number of adapted parameters has increased significantly – almost

three-fold in the present context – and therefore convergence time is affected. On the other hand, we now have a single stage of processing, and therefore there is no second stage of which the convergence depends on a first stage having converged already.

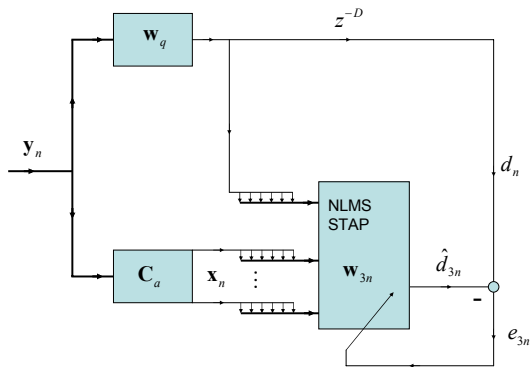


**Fig. 7: Main-aux STAP approach.**

We now change the narrowband pole angle to a fractional frequency of  $0.1\overline{6}$ , so that the new difference frequency relative to the sinusoidal interference is now  $0.13\overline{6}$  (the underscore denotes a repeating digit). With a larger difference frequency any non-Wiener effects will diminish. We also change step-size to 0.05, in order to get convergence to steady-state operation in a few thousand iterations. SIR remains at  $-25$  dB. The SER of the main-aux STAP approach is then directly compared to that of the GSC error smoothing approach, as shown in Fig. 8.

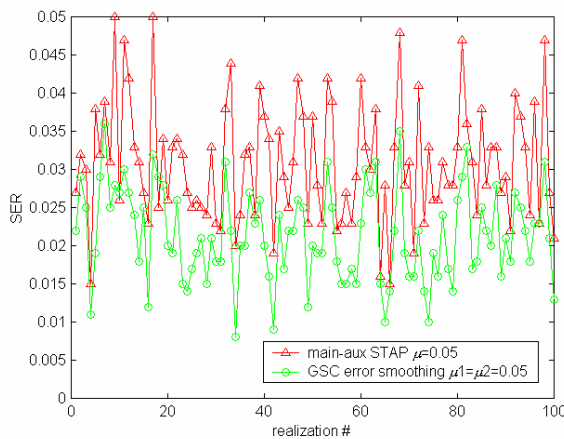


**Fig. 8: Main-aux STAP SER.**

We observe that the SER of the STAP approach – for most realizations – is somewhat higher than the SER performance for the GSC error smoothing approach. The average SER for the GSC error smoothing approach is 0.0213, while for main-aux STAP it is 0.0309.

The main-aux STAP weights behave as shown in Fig. 9.

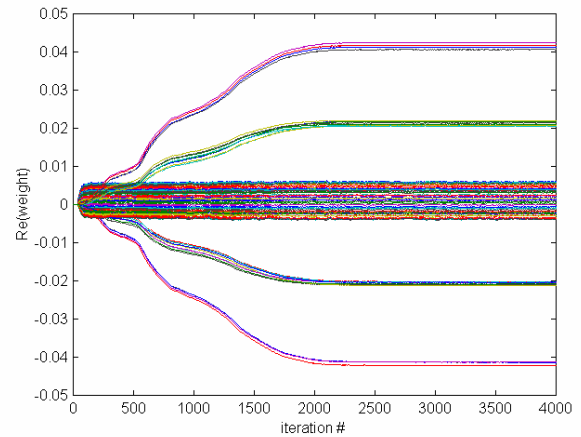


**Fig. 9: Main-aux STAP weight behavior.**

The weights with steady-state amplitudes above 0.01 correspond to operation on the main beam, while those with amplitudes close to zero correspond to operation on the auxiliary beams. All weights are seen to be static in steady state, apart from a small amount of noise. During the transient state, however, the dynamic weight behavior is different, in particular for the auxiliary beam weights. Figure 10 shows a zoomed in look at (some of) the auxiliary beam weights (the behavior of the deleted auxiliary beam weights is typically the same as for those that are shown).

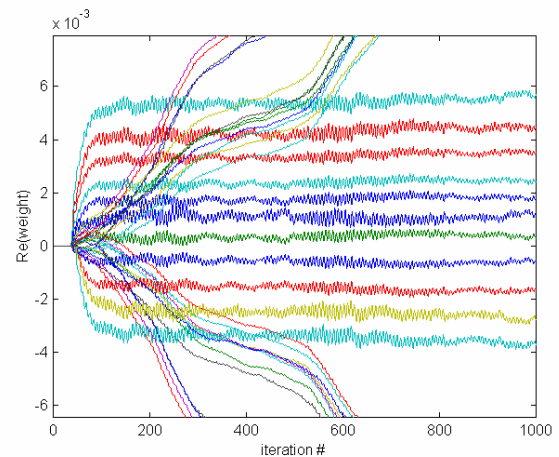


**Fig. 10: Transient aux beam STAP weight behavior.**

The auxiliary beam weights are seen to behave in semi-periodic fashion. In Fig. 11 we zoom in on one of these weights.

We observe approximately 9.5 periods over 70 samples, which corresponds well with a difference frequency of  $0.13\overline{6}$  (9.5 periods in 69.5 samples). Recall the earlier non-Wiener effect in NLMS GSC, where only the auxiliary beam information was input to the adaptive filter, and consequently the dynamic weight behavior was persistent. In main-aux STAP the semi-periodic weight behavior during the transient serves to produce a small

error early on, while ultimately the semi-periodic dynamic behavior is no longer necessary when the error can remain small as a result of the convergence of the main beam STAP weights (at about iteration 2100).

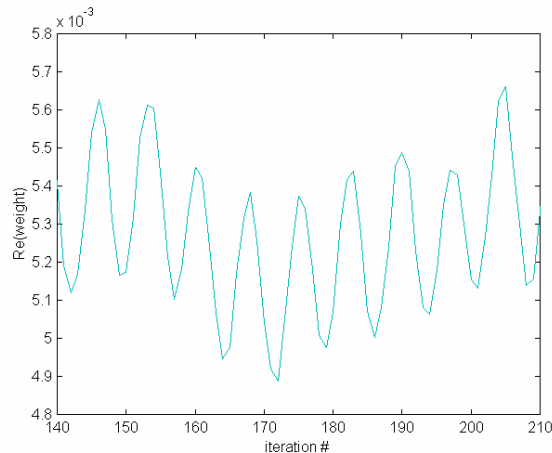


**Fig. 11: Transient aux beam STAP weight behavior.**

An interpretation of the NLMS algorithm at maximum step-size of one is that the norm of the weight vector increment is minimized while finding the new weight vector in the manifold of weight vectors that produces an a posteriori error of zero [8]. Some of this emphasis on minimizing the weight vector increment remains when the step-size is smaller, and ultimately leads to a constant weight vector (increment norm of zero) when one exists.

## 6. Conclusion

We have shown that non-Wiener effects in adaptive filtering, in particular in NLMS, can produce beneficial performance enhancements in the generalized sidelobe canceler scenario. The benefit is that main beam narrowband interference can be mitigated, even though no information about the latter is present in the auxiliary beams. The beneficial non-Wiener effect can result from changing the adaptation step-size from small to large. Further improvements in mitigating main beam

interference were shown to result from adding a second stage adaptive filter aiming to estimate – and subtract – the narrowband interferer. Instead of creating a second stage adaptive filter, a single-stage space-time adaptive processor operating on gapped tapped delay line information from the main and auxiliary beams simultaneously showed performance competitive with that of the two-stage approach consisting of a generalized sidelobe canceler followed by error smoothing.

## References

- [1] J. G. Proakis, Digital Communications, New York, New York: McGraw-Hill, 1983.
- [2] B. Sklar, Digital Communications: Fundamentals and Applications, Englewood Cliffs, New Jersey: Prentice-Hall, 1988.
- [3] B. Widrow and S. D. Stearns, Adaptive Signal Processing, Englewood Cliffs, New Jersey: Prentice-Hall, 1985.
- [4] N. L. Owsley, Chapter 3 in Array Signal Processing, Ed. S. Haykin, Englewood Cliffs, New Jersey: Prentice-Hall, 1985.
- [5] A. A. (Louis) Beex, Rachel E. Goshorn, and James R. Zeidler, Improved look-direction interference suppression in NLMS generalized sidelobe canceler using dynamic weight behavior, *Fifth IASTED International Conference on Signal and Image Processing (SIP 2003)*, Honolulu, Hawaii, 13-15 August 2003.
- [6] M. Reuter, K. Quirk, J. Zeidler, and L. Milstein, Nonlinear effects in LMS adaptive filters, *Proc. Symp. 2000 on Adaptive Systems for Signal Processing, Communications and Control*, pp. 141-146, Lake Louise, Alberta, October 2000.
- [7] A. A. (Louis) Beex and James R. Zeidler, “Steady-State Dynamic Weight Behavior in (N)LMS Adaptive Filters,” Chapter 9 in Advances in Least Mean Square Adaptive Filters, eds. S. Haykin and B. Widrow, John Wiley & Sons, July 2003.
- [8] G. C. Goodwin and K. S. Sin, Adaptive Filtering, Prediction, and Control, Prentice-Hall, 1984.